Channel Capacities for Different Antenna Arrays with Various Transmitting Angles in Tunnels

Chien-Ching Chiu & Su-Ei Wu

Wireless Personal Communications
An International Journal

ISSN 0929-6212

Wireless Pers Commun
DOI 10.1007/s11277-014-1896-7

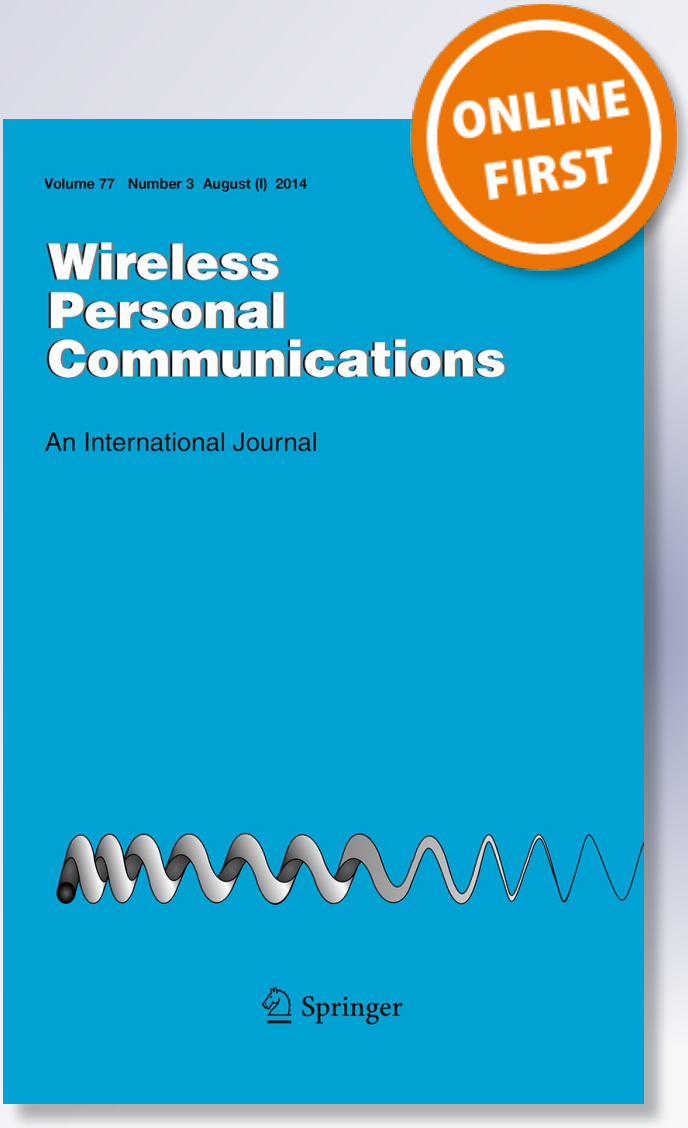

Springer

Wireless Pers Commun
DOI 10.1007/s11277-014-1896-7

Channel Capacities for Different Antenna Arrays with Various Transmitting Angles in Tunnels

Chien-Ching Chiu · Su-Ei Wu

Abstract This paper focuses on the research of channel capacity of multiple-input multiple-output (MIMO) system with different transmitting angles in straight and curvy tunnels. A ray-tracing technique is developed to calculate channel frequency responses for tunnels, and the channel frequency response is further used to calculate corresponding channel capacity. The channel capacities are calculated based on the realistic environment. The channel capacities of MIMO long term evolution system using spatial and polar antenna arrays by different transmitting angles are computed. Numerical results show that, The channel capacity for transmitting angle at 15° is largest compared to the other angles in the tunnels. Moreover, the channel capacity of polar array is better than that of spatial array both in the straight and curvy tunnels. Besides, the channel capacity for the tunnels with traffic is larger than that without traffic. Finally, it is worth noting that in these cases the present work provides not only comparative information but also quantitative information on the performance reduction.

Keywords MIMO-LTE · Ray-tracing approach · Channel capacity · Spatial array and polar array

1 Introduction

MIMO technology has attracted huge attention in wireless communications, due to its ability of offering significant increase in data throughput and link range without additional bandwidth or transmit power in the presence of multi-path scattering. These techniques can be very useful in special environments such as tunnels. However, spatial fading correlation has its direct effect on the channel capacity of indoor MIMO systems. Therefore, multiple antenna arrays used in the transmitter and the receiver should be accurately designed to reduce the spatial correlation, achieve higher capacity and provide more spatial degrees of freedom [1–6].

C.-C. Chiu (✉) · S.-E. Wu
Department of Electrical Engineering, Tamkang University, Tamsui, Taiwan, ROC
e-mail: chiu@ee.tku.edu.tw

Published online: 01 July 2014

In the past, most papers discussed the channel parameters of curvy and straight tunnels [7–12]. Furthermore, spatial antenna array deployment is used for MIMO in most researches. However, polar array antenna deployment is more suitable than spatial antenna array deployment in some scenarios. Channel capacity is an average performance criteria for digital wireless communication system. In this paper, channel capacities of MIMO-LTE system [12,13] by using spatial and polar antenna arrays at different transmitting angles are computed. The most suitable transmitting angle is investigated. The channel capacities for spatial array (SA) and polar array (PA) are compared in the straight and curvy tunnels with and without traffic.

This paper aims at using SBR/Image method to study the channel capacity for tunnels. The remainder of this paper is organized as follows. In Sect. 2, system description and channel modeling are presented. Several numerical results are included in Sect. 3, while Sect. 4 concludes the paper.

2 Channel Modeling and System Description

2.1 System Description

A time-invariant narrowband MIMO system can be described as follows:

$$\mathbf{Y} = \mathbf{HX} + \mathbf{W} \tag{1}$$

where $\mathbf{Y}, \mathbf{X}, \mathbf{W}$ denote the $N_r \times 1$ received signal vector, the $N_t \times 1$ desired transmitted signal vector, and the $N_r \times 1$ zero mean additive white Gaussian noise vector at a symbol time, respectively. In the equation, $\mathbf{H}$ is the $N_r \times N_t$ channel matrix for desired signal.

The channel capacity of narrowband MIMO system for $N_r \leq N_t$ at the fth frequency component can be rewritten as follows:

$$C_f^{NB} = B \log_2 \left[\det \left(I + \frac{SNR_t}{N_t} HH^* \right) \right] \tag{2}$$

Similarly, the channel capacity for $N_t \leq N_r$ can be expressed as

$$C_f^{NB} = B \log_2 \left[\det \left(I + \frac{SNR_t}{N_t} H^* H \right) \right] \tag{3}$$

For convenience, the eigenmatrix R_H is defined as follows:

$$R_H = \begin{cases} HH^* \text{ if } N_r \leq N_t \\ H^* H \text{ otherwise} \end{cases} \tag{4}$$

Then, the channel capacity can be expressed as follows:

$$C_f^{NB} = B \log_2 \left[\det \left(I + \frac{SNR_t}{N_t} R_H \right) \right] \tag{5}$$

where SNR_t denotes the ratio of the total transmitting power of the desired signal to noise power.

An $N_t \times N_r$ LTE system can be represented by the three-dimensional matrix $\mathbf{H}^{LTE} \in C^{N_r \times N_t \times N_f}$ such that $\mathbf{H}^{LTE} = [\mathbf{H}_f^{NB}]$, f $= 1, 2, \ldots, N_f$, where H_f^{NB} is defined as a flat-fading channel matrix of narrowband MIMO system at the fth frequency component and N_f is the number of discrete frequency components of LTE system. When the frequency components of a wideband channel are uncorrelated to each other, it is possible to divide the wideband channel into several narrowband channels [11,12]. As a result, MIMO capacity of

LTE systems can be seen as the summation of several MIMO capacities of NB systems at every discrete frequency component, and it can be expressed as follows:

$$C^{LTE} = \sum_{f=1}^{N_f} C_f^{NB} \text{ (bits/s)} \tag{6}$$

where C_f^{NB} is the MIMO capacity of NB systems at the fth frequency component. More generally, the channel capacity (spectral efficiency) can be written as

$$C_{SE}^{LTE} = \frac{C^{LTE}}{BW} \text{ (bits/s/Hz)} \tag{7}$$

This equation expresses the achievable spectral efficiency through the MIMO channel and BW is the bandwidth of LTE system.

Calculated channel capacity after normalized can be remove the path loss. The normalization can separate the problems of calculating link-budget power and of studying the effects of channel fading. In general, channel matrix H of MIMO-LTE systems can be normalized to the new matrix $\hat{H}$ as follows:

$$\hat{H} = \frac{H}{H_n} \tag{8}$$

where $H_n$is defined as follows:

$$H_n = \sqrt{\frac{1}{N_t N_r N_f} \sum_{f=1}^{N_f} \sum_{i=1}^{N_r} \sum_{j=1}^{N_t} \left| h_{ij,f} \right|^2} \tag{9}$$

where $\left| h_{ij,f} \right|$ is the channel amplitude gain from the jth transmitting antenna to the ith receiving antenna at the fth frequency component. After normalizing process, Eq. (5) combining Eq. (7) can be rewritten as follow:

$$C_{SE}^{LTE} = \frac{1}{BW} \sum_{f=1}^{N_f} B \log \left(\det \left(I + SNR_r \times \hat{R}_{Hf} \right) \right) \tag{10}$$

where $SNR_r = \frac{SNR_t}{N_t} \times H_n^2$ denotes the ratio of average receiving signal power to noise power on each receiving antenna and $\hat{R}_{H,f}$ is the normalized eigenmatrix at the fth frequency component.

2.2 Channel Modeling

The shooting and bouncing ray (SBR)/Image method can deal with high frequency radio wave propagation in complex indoor environments [14,15]. It conceptually assumes that many triangular ray tubes are shot from the transmitting antenna (TX), and each ray tube, bouncing and penetrating in the environments is traced in the indoor multi-path channel. If the receiving antenna (RX) is within a ray tube, the ray tube will have contributions to the received field at the RX, and the corresponding equivalent source (image) can be determined. By summing all contributions of these images, we can obtain the total received field at the RX. In real environments, external noise in the channel propagation has been considered. The depolarization yielded by multiple reflections, refraction and first-order diffraction is also taken into account in our simulations.

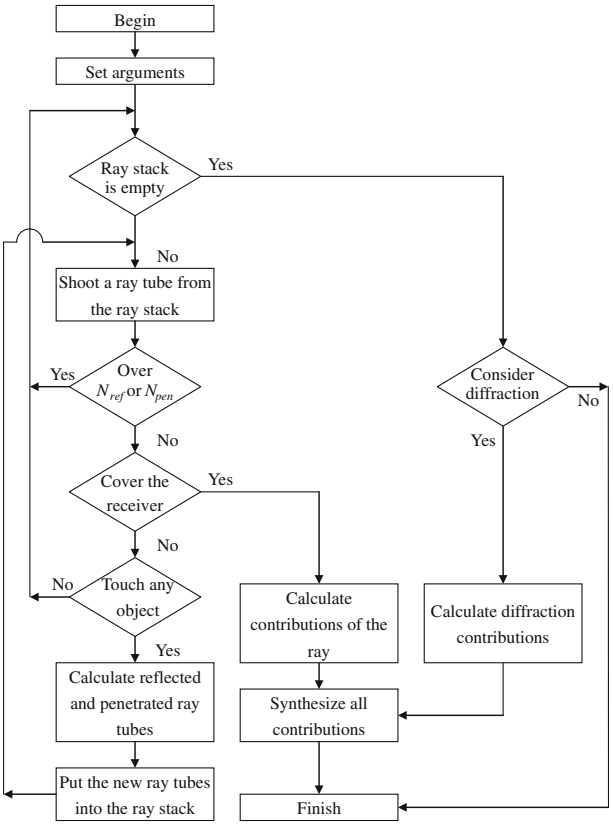

Fig. 1 Flow chart of the ray-tracing process

Using ray-tracing approaches to predict channel characteristic is effective and the approaches are also usually applied to LTE in recent years [16,17]. Thus, a ray-tracing channel model is developed to calculate the channel matrix of MIMO-LTE system. Flow chart of the ray-tracing process is shown in Fig. 1. It conceptually assumes that many triangular ray tubes (not rays) are shot from a transmitter. Here the triangular ray tubes whose vertexes are on a sphere are determined by the following method. First, we construct an icosahedron which is made of 20 identical equilateral triangles. Then, each triangle of the icosahedron is tessellated into a lot of smaller equilateral triangles. Finally, these small triangles are projected on to the sphere and each ray tube whose vertexes are determined by the small equilateral triangle is constructed [18].

By using these images and received fields, the channel frequency response can be obtained as following:

$$\boldsymbol{H}(f) = \sum_{p=1}^{N_p} a_p(f) e^{j\theta_p(f)} \tag{11}$$

where p is the path index, N_p is the number of paths, f is the frequency of sinusoidal wave, $\theta_p(f)$ is the pth phase shift and $a_p(f)$ is the pth receiving magnitude. Note that the channel

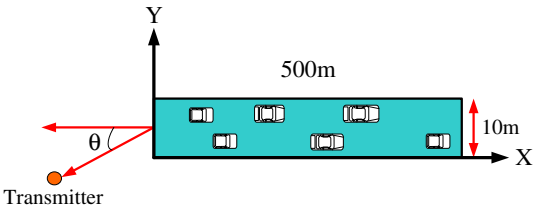

Fig. 2 The *top* view of the straight tunnel with traffic

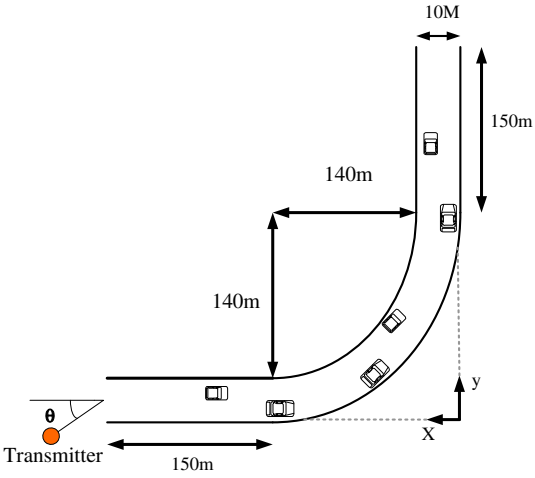

Fig. 3 The top view of the curvy tunnel with traffic

frequency response of LTE systems can be calculated by Eq. (11) in the frequency range of LTE for desired signal.

3 Numerical Results

Let us consider the top view of straight tunnel as shown in Fig. 2, In the figure, dimensions of the straight tunnels is 500 m (Length) × 10 m (Width) × 6 m (Height). Figure 3 shows the curvy tunnels. The transmitter antenna Tx is located at the entrance of the tunnel with distance 10 m and different transmitting angles as shown in Figs. 2 and 3. The transmitter is with the fixed height of 3.5 m. Moreover, the locations of receiving antenna with a fixed height of 1 m are uniformly distributed in tunnel and there are total 300 receiving points. Furthermore, two different antenna arrays, spatial array (SA) and polar array (PA), are considered as shown in Fig. 4a, b respectively. The antenna spacing for spatial arrays is 21.4 cm which is about half wavelength to correspond the center frequency 700 MHz of MIMO-LTE.

A ray-tracing technique is developed to calculate the channel frequency response from 675 to 725 MHz with frequency interval of 200 KHz. i.e., 246 frequency components are used. The maximum number of bounces is set to be five, and the convergence is confirmed.

3.1 Straight Tunnel

The average capacities at SNRr = 20 dB for different transmit angles of Spatial Array Multiple-Input Multiple-Output (MIMO-SA) and Polar Array Multiple-Input Multiple-Output (MIMO-PA) in the straight tunnel are shown in Fig. 5. It is clear the channel capacity

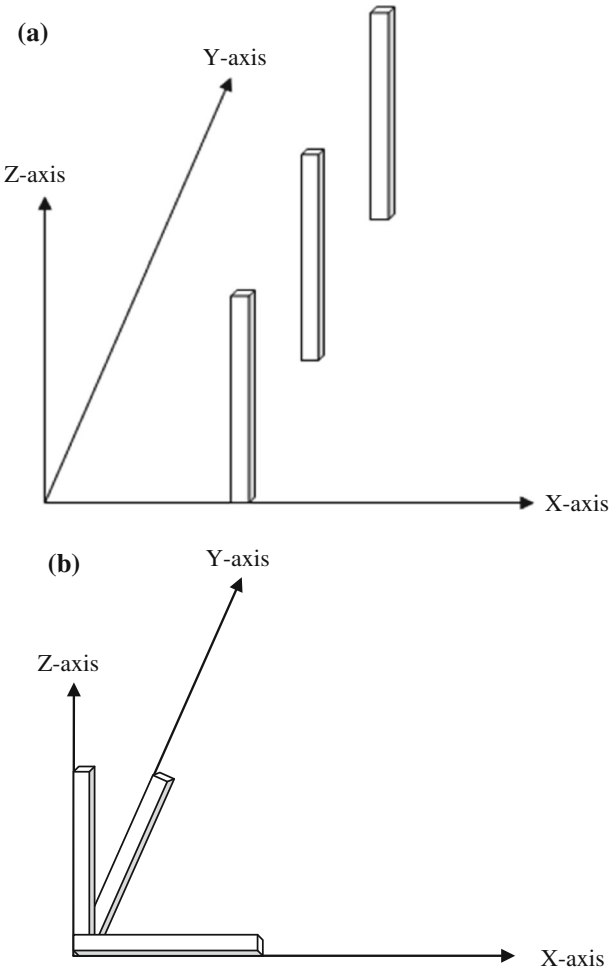

Fig. 4 **a** Spatial linear array. **b** Tri-polar array

for the transmit angle of 15° is the largest. This is because more rays can shoot into the tunnel at this angle. The average channel capacity at transmitting angle of 15° without traffic for MIMO-PA and MIMO-SA is 13.26 and 11.66 bits/s/Hz, respectively. The average channel capacity with traffic for MIMO-PA and MIMO-SA is 15.05 and 13.76 bits/s/Hz, respectively. It is seen that the capacity for MIMO-SA is smaller than that for MIMO-PA. The reason is that the correlation of MIMO-SA is larger than that of MIMO-PA. In other words, when the MIMO-SA system breaks a multipath channel into several individual spatial channels to enhance the capacity, the individual spatial channels are affected by each other. As a result, the correlation of MIMO-SA is stronger compared to MIMO-SA. In contrast to MIMO-SA, MIMO-PA breaks a multipath channel into several individual channels to enhance the channel capacity by using polarization. Numerical results show that changing the polarization can improve the channel capacity effectively. It is also clear that the capacity for the tunnel with traffic is larger than that without traffic, no matter what MIMO-SA or MIMO-PA is employed. This is due to the fact that the multipath effect becomes serious when the tunnel is with traffic.

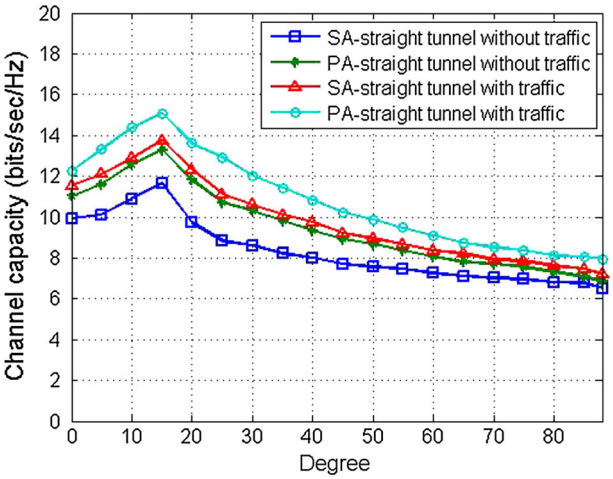

Fig. 5 The average capacities of MIMO-SA and MIMO-PA system at SNRr = 20 dB for different transmitting angles in the straight tunnel

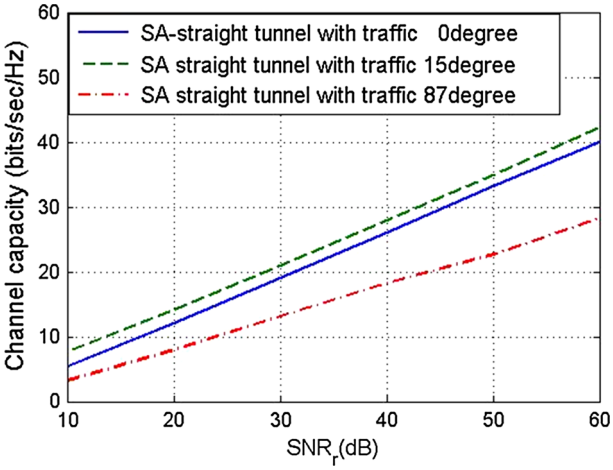

Fig. 6 The average capacities of MIMO-SA system at transmitting angles of 0°, 15° and 87° for different SNRr in the straight tunnel with traffic

The channel capacities of MIMO-SA at transmitting angles of 0°, 15° and 87° for different SNRr in the straight tunnel with traffic are plotted in Fig. 6. It is seen that the channel capacity is almost linearly proportional to single to noise ratio. The average channel capacity of MIMO-SA at SNRr = 30 dB for transmit angles of 0°, 15° and 87° is 19.01, 20.91 and 13.21 bits/s/Hz, respectively. Similarly, the channel capacities of MIMO-PA versus SNRr are shown in Fig. 7. The channel capacity is also linearly proportional to SNRr. The average channel capacity of MIMO-SA at SNRr = 30 dB for transmit angles of 0°, 15° and 87° is 20.15, 22.35 and 15.15 bits/s/Hz, respectively. Compared Figs. 6 and 7, it is observed that the channel capacities for MIMO-PA is larger than those for MIMO-SA when the SNRr is the same, no matter what angles are used.

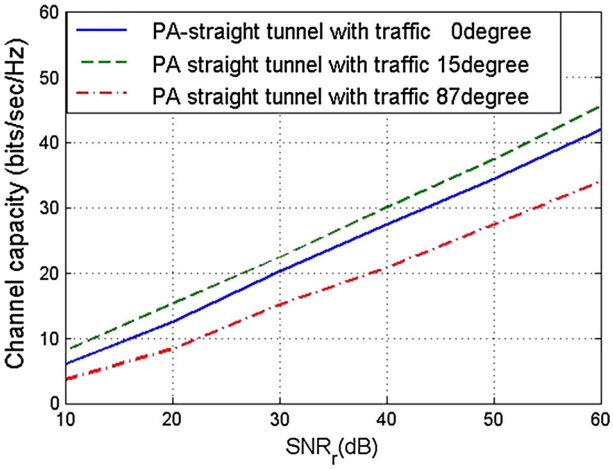

Fig. 7 The average capacities of MIMO-PA system at transmitting angles of 0°, 15° and 87° for different SNRr in the straight tunnel with traffic

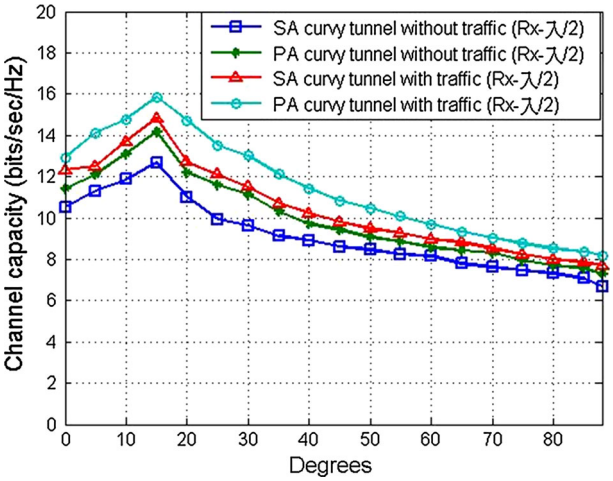

Fig. 8 The average capacities of MIMO-SA and MIMO-PA system at SNRr = 20 dB for different transmitting angles in the curvy tunnel

3.2 Curvy Tunnel

The average capacities of spatial array multiple-input multiple-output (MIMO-SA) and polar array multiple-input multiple-output (MIMO-PA) with different transmitting angles in curvy tunnels are shown in Fig. 8. It is observed that the channel capacity for the transmit angle of 15° is the largest. This is because more rays can shoot into the tunnel at this angle. The average channel capacity of MIMO-PA and MIMO-SA at transmitting angle of 15° in the curvy tunnel without traffic is 14.17 and 12.66 bits/s/Hz, respectively. The average channel capacity with traffic for MIMO-PA and MIMO-SA is 15.86 and 14.92 bits/s/Hz, respectively. It is found that the capacity for MIMO-PA is larger than that for MIMO-SA. It is clearly seen that the capacity without traffic is smaller than that with traffic for both MIMO-SA and

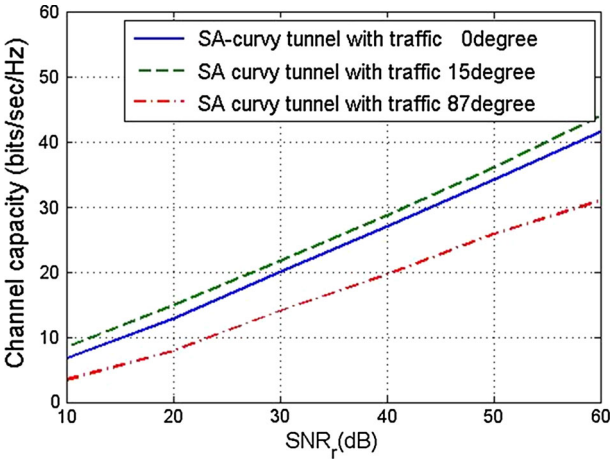

Fig. 9 The average capacities of MIMO-SA system at transmitting angles of 0°, 15° and 87° for different SNRr in the curvy tunnel with traffic

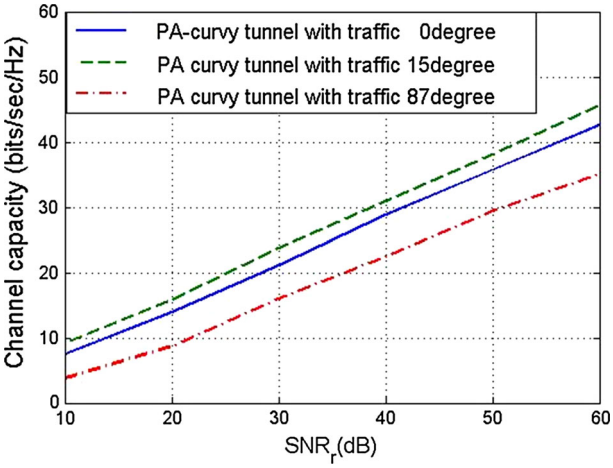

Fig. 10 The average capacities of MIMO-PA system at transmitting angles of 0°, 15° and 87° for different SNRr in the curvy tunnel with traffic

MIMO-PA. From Figs. 5 and 8, it is seen that the capacity for straight tunnel are smaller than that for curvy tunnel, no matter what arrays are employed. This is dut to the fact that the multipath effect for the straight tunnel is less severe than that for the curvy tunnel.

The channel capacities of MIMO-SA at transmitting angles of 0°, 15° and 87° for different SNRr in the curvy tunnel with traffic are plotted in Fig. 9. It is seen that the channel capacity is almost linearly proportional to single to noise ratio. The average channel capacity of MIMO-SA at SNRr = 30 dB for transmit angles of 0°, 15° and 87° is 20.35, 21.75 and 14.05 bits/s/Hz, respectively. Similarly, the channel capacities of MIMO-PA versus SNRr are shown in Fig. 10. The channel capacity is also linearly proportional to SNRr. The average channel capacity of MIMO-SA at SNRr = 30 dB for transmit angles of 0°, 15° and 87° is 21.11, 23.82 and 16.01 bits/s/Hz, respectively. From Figs. 9 and 10, it is clear that the channel

capacities for MIMO-SA is smaller than those for MIMO-PA when the SNRr is the same, no matter what angles are used.

4 Conclusion

A research of the channel capacity of MIMO-SA and MIMI-PA in various tunnels with different transmitting angle has been presented. By using the ray-tracing model of these multi-path channels, the channel frequency response for MIMO communication systems is calculated. The frequency responses are used to calculate the channel capacity for spatial and polar antenna arrays. Numerical results show that the channel capacities for various tunnels and different transmitting angles of MIMO-SA and MIMI-PA has different results. The channel capacity for transmitting angle of 15° is the best. It is also found that the channel capacity of MIMO-PA is better than that of MIMI-SA in both straight and curvy tunnels. Moreover, the channel capacity for the curvy tunnel is larger than that for the straight tunnel. Finally, it is worth noting that in these cases the present work provides not only comparative information but also quantitative information on the performance reduction.

References

1. Durgin, G. D. (2003). *Space-time wireless channels*. New Jersey: Prentice Hall PTR.
2. Tse, D., & Viswanath, P. (2005). *Fundamentals of wireless communication*. UK: Cambridge University Press.
3. Paul, B. S., & Bhattacharjee, R. (2008). MIMO channel modeling: A review. *IETE Technical, 25*(6).
4. Oestges, C., & Clerckx, B. *Mimo wireless communications*.
5. Telatar, I. E. (1999). Capacity of multi-antenna Gaussian channels. *European Transactions on Telecommunications*, *10*, 585–595.
6. Foschini, G. J., & Gans, M. J. (1998). On limits of wireless communications in a fading environment when using multiple antennas. *Wireless Personal Communication*, *6*, 311–335.
7. Hrovat, A., Kandus, G., & Javornik, T. (2010). Four-slope channel model for path loss prediction in tunnels at 400 MHz. *IET Microwaves, Antennas and Propagation*, *4*, 571–582.
8. Molina-Garcia-Pardo, J. M., Rodriguez, J.-V., & Juan-Llacer, L. (2004). MIMO capacity at 2.1GHz while entering tunnels. *IEEE Vehicular Technology Conference*, *1*, 14–16.
9. Valdesueiro, J. A., Izquierdo, B., & Rome, J. (2010). MIMO channel measurement campaign in subway tunnels. In Proceedings of the Fourth European Conference on Antennas and Propagation (EuCAP), Barcelona, Spain, April 12–16, 2010, 1–4.
10. Izquierdo, B., Capdevila, S., Jofre, L., & Romeu, J. (2007). Evaluation of MIMO capacity in train tunnels. *Antennas and Propagation Society International Symposiun 2007 IEEE*, June 2007, pp. 1365–1368.
11. Briso-Rodriguez, C., Cruz, J. M., & Alonso, J. I. (2007). Measurements and modeling of distributed antenna systems in railway tunnels. *IEEE Transactions on Vehicular Technology*, *56*(5), 2870–2879.
12. Chung, J.-Y., Yang, T., & Lee, J. Low correlation MIMO antenna for LTE 700MHz band. *IEEE international conference on acoustics, speech, and signal processing*, pp. 2202–2204.
13. Gentile, C., Golmie, N., Remley, K. A., Holloway, C. L., Young, W. F. (2010). A channel propagation model for the 700MHz band. In Proceedings of IEEE International Conference on Communications, ICC 2010, Cape Town, South Africa, May 23–27, 2010.
14. Chen, S. H., & Jeng, S. K. (Aug. 1996). SBR image approach for radio wave propagation in tunnels with and without traffic. *IEEE Transactions on Vehicular Technology*, *45*(3), 570–578.
15. Chen, S. H., & Jeng, S. K. (1995). An SBR/image approach for indoor radio propagation in a corridor. *IEICE Transactions on Electronics*, *E78–C*(8), 1058–1062.
16. Xiao, P., Lin, Z., & Colin, C. (2010). Analysis of channel capacity for LTE MIMO systems. *Vehicular Technology Conference Fall (VTC 2010-Fall), 2010 IEEE 72nd*, pp. 1–6.
17. Mellios, E., Hilton, G. S, & Nix, A. R. Ray-tracing urban picocell 3D propagation statistics for LTE heterogeneous networks. *Antennas and propagation (EuCAP), 2013 7th European conference on publication year: 2013*, pp. 4015–4019.

18. Zhang, Y. (2004). Ultra-wide bandwidth channel analysis in time domain using 3-D ray tracing. *High frequency postgraduate student colloquium of IEEE,* Sept. 2004, pp. 189-194

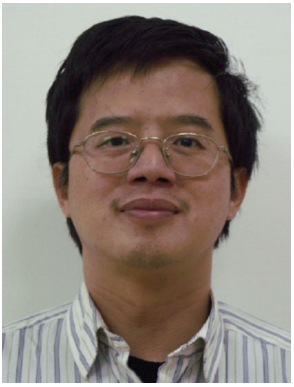

Chien-Ching Chiu received his B.S.C.E. degree from National Chiao Tung University, Hsinchu, Taiwan, in 1985 and his M.S.E.E. and Ph.D. degrees from National Taiwan University, Taipei, in 1987 and 1991, respectively. From 1987 to 1989, he was a communication officer with the ROC Army Force. In 1992 he joined the faculty of the Department of Electrical Engineering, Tamkang University, where he is now a professor. From 1998 to 1999, he was a visiting scholar at the Massachusetts Institute of Technology, Cambridge, and the University of Illinois at Urbana-Champaign. He is a visiting professor with the University of Wollongong, Australia, in 2006. Moreover, he was a visiting professor with the University of London, United Kingdom, in 2011. His current research interests include microwave imaging, numerical techniques in electromagnetics, indoor wireless communications, and ultra wide band communication systems. He has published more than 120 journal papers on inverse scattering problems, communication systems and optimization algorithms.

Su-Ei Wu was born in Taipei, Taiwan, Republic of China, on October 02, 1988. He received the M.S.E.E. degree from Tamkang University in 2013, and now is working toward Ph.D degrees in the Department of Electrical Engineering, National Taipei University of Technology. His current research interests include indoor wireless communication systems, LTE systems, and MIMO systems.